25th ABCM International Congress of Mechanical Engineering
October 20-25, 2019, Uberlândia, MG, Brazil

COB-2019-2386
GLOBAL DYNAMIC ANALYSIS OF A SPAR WIND TURBINE USING THE NONLINEAR NORMAL MODES

Nicaretta, G. A.
Gavassoni, E.
Universidade Federal do Paraná, Department of Civil Construction, Curitiba, Brazil
gabrielarmandonicaretta@yahoo.com;
gavassoni@ufpr.br;

Abstract. *The energy demand growth to sustain economic expansion and social development is a major challenge. Wind energy has been increased prominently in the search for renewable energy sources, and is also a reason for studying its untapped potential at offshore areas. In this scenario, floating offshore wind turbines (FOWTs) have been designed to be installed in deep water levels. These facilities are subject to wind and wave loading. Unlike the usual civil construction structures, floating platforms can present significant angular rotations invalidating a linear analysis of the structure. Due to the coupled between the degrees-of-freedom in nonlinear dynamics, it becomes impracticable to use discretization schemes-based programs without large numerical capacity. However, the use of reduced models based on the concept of nonlinear normal modes (NNMs) can be used for a preliminary analysis. The NNMs can be viewed as nonlinear extension of their counterpart linear modes. The invariant manifolds method is used in the work to obtain the reduced order models (ROM) of a NREL 5-MW Baseline Wind Turbine installed on a Spar Buoy platform. ROM are used to study the nonlinear dynamic behavior of the structure. The phase space, frequency-energy and frequency-amplitude curves are obtained for the two nonlinear normal modes of the system. Some nonlinear phenomena such hardening and softening behavior are observed. The ROM results are compared to the benchmark solution, obtained via the numerical integration of the full system of equation of motion. This comparison confirms that the nonlinear normal modes can be used to study the global nonlinear dynamics of the system.*

Keywords: *Offshore structures, Renewable energy sources, Invariant manifold, Floating platforms, Reduced order models.*

1. INTRODUCTION

Historically, the main energy sources of electricity in Brazil were hydroelectric and thermoelectric. The first one is the main source of electric power in Brazil, and the country has stood out in the world as the main generator of this source. The other is generally used when there is low production coming from hydroelectric plants, which is more expensive and nonrenewable energy source.

Regarding this scenario, it is necessary to diversify the energy matrix of the country. the generation of energy from wind turbines appears as a viable alternative to other sources of energy. This source, besides being renewable, presents great growth potential, not only in onshore regions, but also in offshore regions. The use of wind energy only began to be significant in relation to other sources from the last decade. In 2017, Brazil ranked eighth in the world ranking of installed production capacity of (GWEC, 2018), however, the production of offshore wind from Brazil is insignificant.

The use of offshore wind turbines, which have higher speeds winds, compared to coastal zones, consists of an ideal source of renewable energy (Wang et al. 2018). However, the most critical aspect in the development and expansion of offshore wind energy lies in the viability of the substructure, defined as the supporting part of the structure. The adaptability of substructures to offshore wind turbines is fundamentally limited by the depth of water, geotechnical conditions and size of the wind turbine (Wang et al, 2018). The deep water condition imposes the use of floating platforms anchored by long cables at the seabed.

Floating platforms are generally divided into 3 categories: Tension Leg Platforms (TLP), barge and spar. Spar is platform that achieve stability by using ballast weights hung below a central buoyancy tank which minimize heave and pitching motion (Musial and Butterfield, 2006)**.**

Structures installed in the deep water at great depths are subject to loading imposed by the ocean environment, such as waves, currents and winds, and unlike the usual civil construction structures, angular deviations could be significant, invalidating a linear analysis.

Due to coupling between the degrees-of-freedom, a high computational method effort is required to study the nonlinear dynamical behavior of ocean structures (Gavassoni, 2007). Besides that, parametrical studies are a cumbersome task if

the designer use a full discretization scheme to study the nonlinear oscillations of those systems. An alternative is to use a reduced order model (ROM) to help the designer to gain insight in the nonlinear dynamics of the system before evaluating full specific numerical schemes. The nonlinear normal modes (NNMs) can be used as a properly tool to obtain ROM used in the nonlinear vibration investigation of floating structures (Gavassoni, 2007). NNMs can be regarded as a nonlinear extension of the system's linear vibration modes, however nonlinear systems can exhbit complex behaviors including jumps, bifurcations, subharmonic, superharmonic and internal resonances, modal interactions, chaos and others effects (Kerschen et al. 2009). The concept of NNMs in modal analysis can also be used in additional applications (Vakakis, 1997). The invariant manifold definition (Shaw and Pierre, 1993) of the NNMs are used here and the polynomial expansion method are employed to construct the nonlinear normal modes of the platform analytically. Analytical solutions are an effective tool to perform fast studies that can be used in pre-cycles of design.

The invariant manifold approach was used to derive the NNMs, obtaining a single degree of freedom nonlinear modal oscillator for each NNM. The domain of validity of each modal oscillator was defined by comparing the responses obtained by numerical integration in the phase space of the system. The harmonic balance method was used to study nonlinear features of the system in free vibration such frequency-amplitude and frequency energy dependence.

2. STRUCTURAL MODEL AND FORMULATION

The used structural model of a floating offshore wind turbine (FOWT) is to assume a single rigid body with point mass and inertial characteristics. This problem is governed by a six degrees of freedom system: three translational motions (surge, sway, and heave); and three rotational (roll, pitch, and yaw). It has been shown in other studies (Jonkman, 2007) that the pitching degrees of freedom causes large bending moments in the tower. Therefore the model includes two pitch degrees-of-freedom: θ_1 is the rotational angle of the spar substructure and θ_2 is the tower rotational angle, both angles are related about the vertical axis. The universal hinge connecting the tower to the spar is chosen as the reference system origin. Figure 1 shows the structural model and the main geometrical and structural parameters, whose value are presented in Tab. 1.

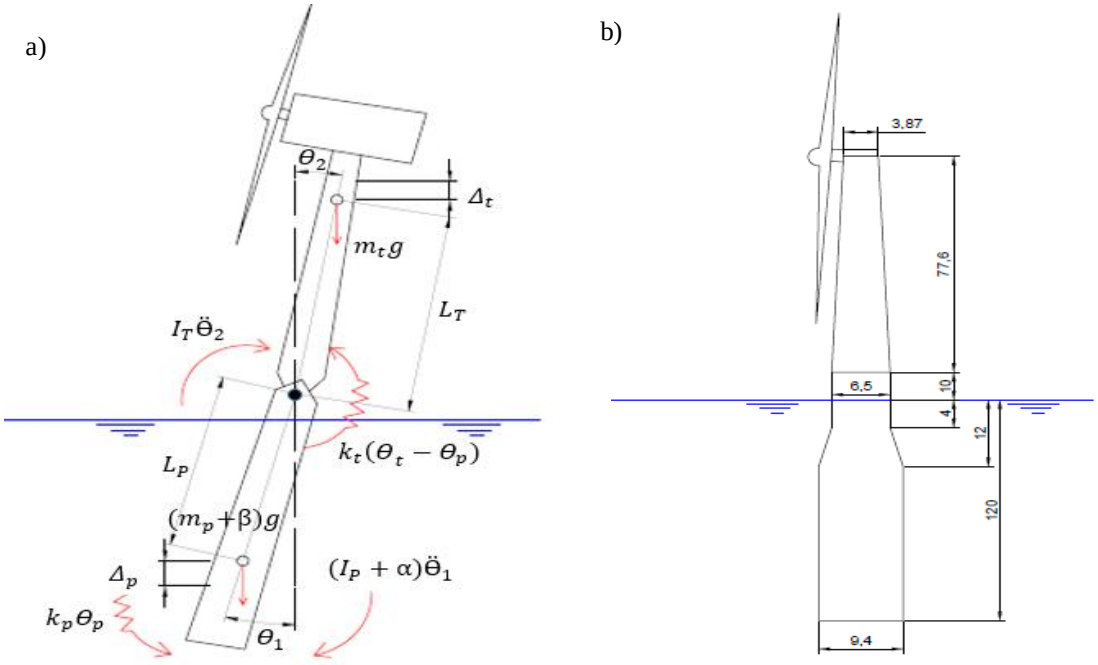

Figure 1: a) Structural model; b) Main dimensions (in meters) of the FOWT

Table 1. Parameters used in structural analysis
(Jonkman, 2010), (Harriger, 2011) e (Jonkman and Musial, 2010)

Symbol	Parameter	Value	Unit
I_P	Spar platform pitching moment of inertia	7,87E+10	kg.m²
I_T	Tower pitching moment of inertiga	2,49E+09	kg.m²
k_P	Spar pitching stiffness including hydrostatic restoring moments	5,00E+09	N.m
k_T	Tower structural stiffness and modeled as a rotary spring at the base of the rigid body	4,60E+08	N.m
m_P	Barge mass including ballast	7,47E+06	kg
m_T	Tower, nacelle and rotor mass	6,00E+05	kg
g	acceleration of gravity	9,81E+00	m/s²
α	Spar platform pitching added mass	3,80E+10	kg.m²
β	Spar platform added mass	7,98E+06	kg
L_P	Spar center of mass location	9,99E+01	m
L_T	Overall (tower, nacelle and rotor) center of mass location	5,92E+01	m

The tower used in the model consists of a 5 MW reference turbine from the National Renewable Energy Laboratory (NREL), of the same model presented in the document by Jonkman (2010). The base of the tower is leased 10 m above the sea level, and its shape is a hollow cone, in which the diameter and thickness vary linearly. For simplicity, when calculating the center of mass and moment of inertia of the system, the rotor and the nacelle were considered as punctual masses located at the top of the tower. The system is composed of two rotational springs with constant stiffness, k_P is relative to the base of platform considering the linear hydrostatic-restoring effects and k_T is at the junction of the tower and platform. The mass of the tower is denoted by m_T and the distance from the center of mass to the origin of the system is indicated by L_T. For the platform the mass is denoted by m_P, with added mass of appointed by β, and distance from the center of mass to the origin of the system L_P. The inertia of the tower is denoted by I_T, for the platform the inertia is given by I_P, with added inertia of α.

The total potential energy of the system in the dynamic configuration is given by:

$$\Pi = U - W; \tag{1}$$

where U represents the elastic potential energy and W is the work of the external loads, namely work of the platform weight and the tower weight. The elastic potential energy can be written as:

$$U = \frac{1}{2}k_P(\theta_1)^2 + \frac{1}{2}k_T(\theta_2 - \theta_1)^2. \tag{2}$$

The work of the platform weight (W_P) and the work of tower weight (W_T) are given, respectively, by:

$$W_P = -(m_P + \beta)gL_P(1 - \cos(\theta_1)); \tag{3}$$

$$W_T = m_T g L_T(1 - \cos(\theta_2)); \tag{4}$$

where g is the acceleration of gravity. By substituting Eqs. (2), (3) and (4) in Eq. (1) one can obtain:

$$\Pi = \frac{1}{2}k_P(\theta_1)^2 + \frac{1}{2}k_T(\theta_2 - \theta_1)^2 + (m_P + \beta)gL_P(1 - \cos(\theta_1)) - m_T g L_P(1 - \cos(\theta_2)). \tag{5}$$

The kinetic energy of the structure depends only on the velocity of the two rotational degree of freedom and the moment of inertia of rigid bodies. The following relation can be used to calculate the kinetic energy:

$$T = \frac{(I_P + \alpha)\dot{\theta}_1{}^2}{2} + \frac{I_T\dot{\theta}_2{}^2}{2}. \tag{6}$$

The dot above the variables stands for its time derivative. By using Hamilton Principle, i.e:

$$\int_{t_1}^{t_2} \delta(T - \Pi)\, dt = 0; \tag{7}$$

where δ is the symbol used to represent the variation, and t is the time variable. Using variational techniques, one can arrive at the following Euler-Lagrange system:

$$\frac{\partial L_g}{\partial \theta_1} - \frac{d}{dt}\left(\frac{\partial L_g}{\partial \dot{\theta}_1}\right) = 0; \tag{8}$$

$$\frac{\partial L_g}{\partial \theta_2} - \frac{d}{dt}\left(\frac{\partial L_g}{\partial \dot{\theta}_2}\right) = 0; \tag{9}$$

where L_g is the resulting Lagrangean. Solving the system defined by Eqs. (8) and (9) obtains the equations of motion described below:

$$(I_P + \alpha)\ddot{\theta}_1 + k_P(\theta_1) + k_t(\theta_1) - K_t(\theta_2) + (m_p + \beta)gL_P sen(\theta_1) = 0; \tag{10}$$

$$I_T\ddot{\theta}_2 + k_T(\theta_2) - k_T(\theta_1) - m_T gL_T sen(\theta_2) = 0. \tag{11}$$

The approximate procedure used here is based on the assumption that the system NNMs can be expressed as a Taylor series around the equilibrium configuration. Nonlinearity comes only from the sine term, which is an odd function, and the minimum expnsion to maintain nonlinearity is up to third term, resulting in:

$$(I_P + \alpha)\ddot{\theta}_1 + k_P(\theta_1) + k_t(\theta_1) - K_t(\theta_2) + (m_p + \beta)gL_P(\theta_1) - \frac{1}{6}(m_p + \beta)gL_P(\theta_1)^3 = 0; \tag{12}$$

$$I_T\ddot{\theta}_2 + k_T(\theta_2) - k_T(\theta_1) - m_T gL_T(\theta_2) + \frac{1}{6}m_T gL_T(\theta_2)^3 = 0. \tag{13}$$

3. NONLINEAR NORMAL MODES THEORY

The nonlinear modal analysis performed in this work uses the invariant manifold approach proposed by Shaw and Pierre (Shaw and Pierre, 1993). The nonlinear normal mode, according to the invariant manifold definition, corresponds to a motion bounded by a surface in the system phase space. This surface is tangent, at the equilibrium position, to the eigenspace formed by the linear modes of the linearized underlying problem (Pesheck et al. 2001). The motion corresponding to a single nonlinear mode can be parameterized by the displacement and velocity of a single degree-of-freedom of the system, which is called the master pair. All remaining degrees-of-freedom, called slave coordinates, are related to the master pair via the constraint equations. The constraint equations determine the invariant manifold geometry for a given nonlinear mode.

This work uses the asymptotic mode to derive the nonlinear modes. To use this method the set of nonlinear equations of motion must be re-written as Cauchy first order equations.(Apiwattanalunggarn et al. 2003).

$$\{\dot{\theta}\} = \{y\}, \{\dot{y}\} = \{f\}; \tag{14}$$

where θ_i are the angular displacements and y_i are the corresponding angular velocities of the system. The generalized force vector *{f}* consists of nonlinear moments that in general depend upon *{θ}* and *{y}*.The dot above the variables stands for its first time derivative.

Then a displacement-velocity pair is arbitrarily chosen as the master pair. As an example the platform angular displacement-velocity pair, θ_1 e y_1, are chosen as the master pair:

$$u = \theta_1, v = y_1. \tag{15}$$

The tower slave par is represented in terms of *u* and *v* by the constraint functions (P_2, Q_2):

$$\theta_2 = P_2(u, v), y_2 = Q_2(u, v); \tag{16}$$

where, particularly, $P_1(u,v)=u$, $Q_1(u,v)=v$.

The next step is to eliminate the explicit time dependence of the equations. This is done by performing the time derivatives of the constraint equations. By replacing the time derivative resulting from the chain rule into the equations of motion and by the use of the master pair definitions in Eq. (15) and the slave relations in Eq. (16), the following system of second order partial differential equations is obtained:

$$Q_2(u,v) = \frac{\partial P_2(u,v)}{\partial u} + \frac{\partial P_2(u,v)}{\partial v} f_1\big(u, P_2(u,v), v, Q_2(u,v)\big); \tag{17}$$

$$f_2\big(u, P_2(u,v), v, Q_2(u,v)\big) = \frac{\partial Q_2(u,v)}{\partial u} v + \frac{\partial Q_2(u,v)}{\partial v} f_1\big(u, P_2(u,v), v, Q_2(u,v)\big). \tag{18}$$

The determination of the restraint equations leads to an order reduction of the problem, since their substitution in the original equations of motion results in a single degree-of-freedom nonlinear modal oscillator. Except for a few special cases, there is no closed exact solution for the differential partial equations that govern the invariant manifold expressed by (17) and (18). The solution can be derived in an analytical form using a Taylor series around the equilibrium configuration, taken here for simplicity as $\{\theta_l\} = 0$. Accordingly, the constraint functions can be written up to third order terms as:

$$P_2 = a_{1,2}u + a_{2,2}v + a_{3,2}u^2 + a_{4,2}uv + a_{5,2}v^2 + a_{6,2}u^3 + a_{7,2}u^2v + a_{8,2}uv^2 + a_{9,2}v^3; \tag{19}$$

$$Q_2 = b_{1,2}u + b_{2,2}v + b_{3,2}u^2 + b_{4,2}uv + b_{5,2}v^2 + b_{6,2}u^3 + b_{7,2}u^2v + b_{8,2}uv^2 + b_{9,2}v^3. \tag{20}$$

The substitution of Eqs. (19) and (20) into the equation of motion results in an algebraic system of equations in terms of the constraint equations coefficients a_{ij} and b_{ij} and they can be sequentially solved. The so-obtained solution is valid only locally (Pesheck et al., 2001). and the validity domain is not known a priori, being determined only by comparison with numerical solutions of the original problem.

4. MODAL ANALYSIS

The linear normal modes (LNMs) of the system are obtained by disregarding the nonlinearity terms of the Eqs. (12) and (13). The solution involves solving a generalized eigenvalue problem, resulting in frequencies and vibration modes for each LNM that are presented in Tab. 2.

Table 2. Frequencies and vibration modes of the linear system

	Frequency	Vibration mode	
First LNM	0.19869 (0,031623 Hz)	Θ_1=0,028752	Θ_2=1
Second LNM	0.42628 (0,067845 Hz)	Θ_1=-0,74142	Θ_2=1

The constraint function written up to third order of the two NNMs were obtained, the Eqs. (21) and (22) refer to the first NNM (in-phase) and the Eqs. (23) and (24) refer to the second NNM (out-of-phase), and the resulting sufaces can be compared to the linear manifolds shown in Figure 2 and Figure 3. It shows that in the equilibrium point, where the displacement and velocity of the master coordinate are zero, the two-dimensional invariant manifold of system with the corresponding linear normal modes (LNMs) are tangent.

$$P_2(u,v) = 34{,}77974783u - 238553{,}3904uv^2 - 3762{,}283329u^3; \tag{21}$$

$$Q_2(u,v) = 34{,}77974983v - 238553{,}3904v^3 + 7548{,}570696u^2v. \tag{22}$$

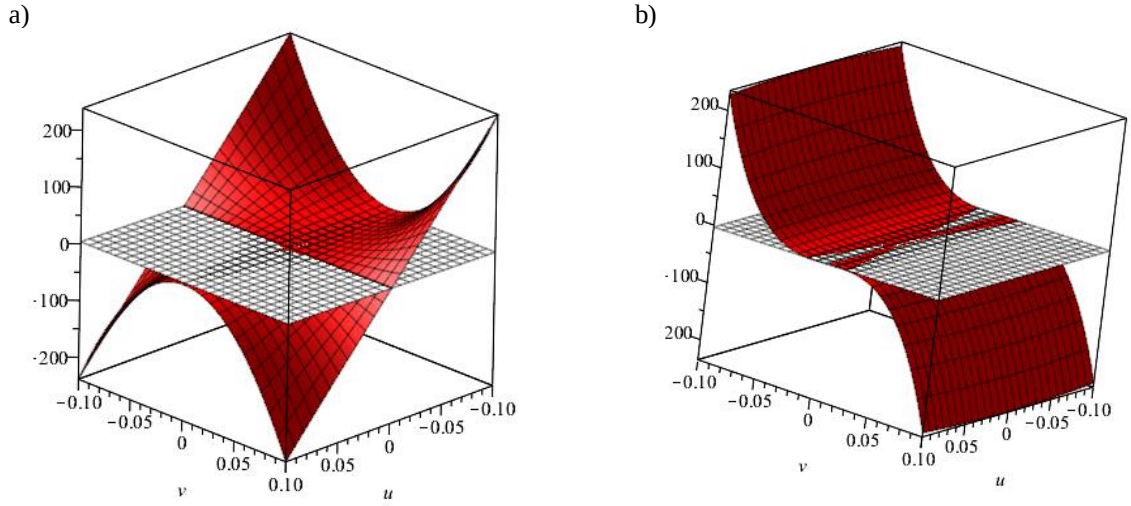

Figure 2: Two-dimensional invariant manifold of the first NNM with the corresponding LNM. a) equation 21; b) equation 22

$$P_2(u,v) = -1{,}348747147u - 0{,}4688442120u^3 - 2{,}282272831uv^2; \tag{23}$$

$$Q_2(u,v) = -1{,}348747147v - 0{,}5770566955u^2v - 2{,}282272831v^3. \tag{24}$$

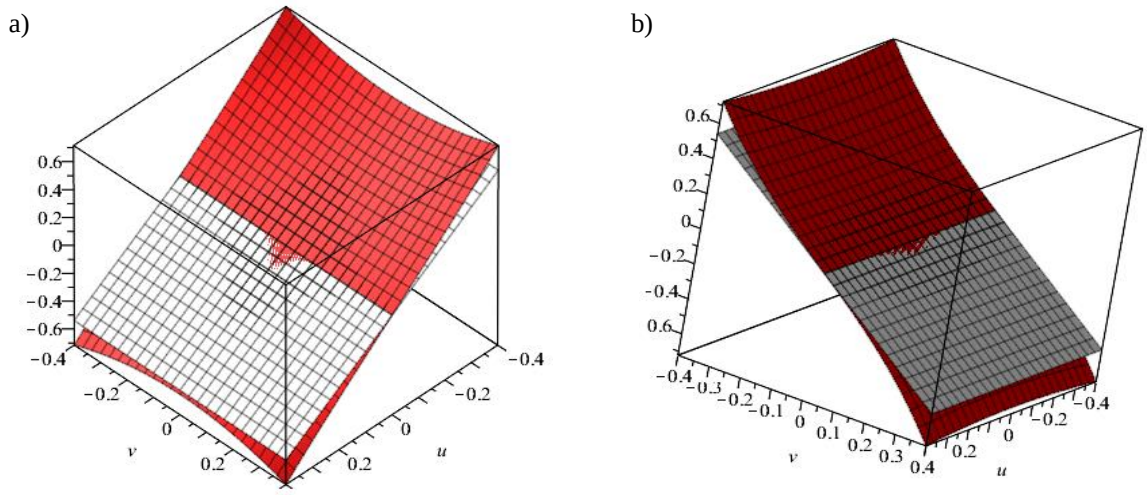

Figure 3: Two-dimensional invariant manifold of the second NNM with the corresponding LNM. a) equation 23; b) equation 24

The effects of nonlinearity are more easily identified in the graphs of the first NNM constraint functions. The constraint functions of the second NNM resemble a plane for larger ranges of displacements and velocities of the master degree of freedom.

It can be obtained two 1-degree of freedom (DOF) oscillators, when the respective constraint equations are substituted in the Eq. (12), written in terms of the modal displacements for the chosen master pair of the platform. The Eqs. (25) and (26) are related respectively to the first NNM and the second NNM.

$$\ddot{u} + 0{,}0394784175u + 14{,}79103655u^3 + 939{,}2187577\dot{u}^2u = 0; \tag{25}$$

$$\ddot{u} + 0{,}1817214684u - 0{,}01976417535u^3 + 0{,}008985633989\dot{u}^2u = 0. \tag{26}$$

The modal oscillators are reduced order systems, which the cubic terms have the opposite sign, in the first NNM it is positive and in the second NNM it is negative, besides having mixed terms of velocity x displacement. Analyzing the linear terms of the Eqs. (25) and (26), both are equal to the square of the vibrations frequencies in rad/s of the linear system. This indicated, as expected, that linearizing the equations of the modal oscillators results in the same equations

of the motion of the decoupled linear system. Therefore, the surface corresponding to the phase space of the nonlinear system is tangent at the point of equilibrium with the plane coming from linear analysis.

Exciting the nonlinear system in the respective NNMs using the constraint equations defined in Eqs. (21) to (24), and comparing with the reference solution obtained by numerical integration, as shown in Fig. 4, it can be observed diferent situations.

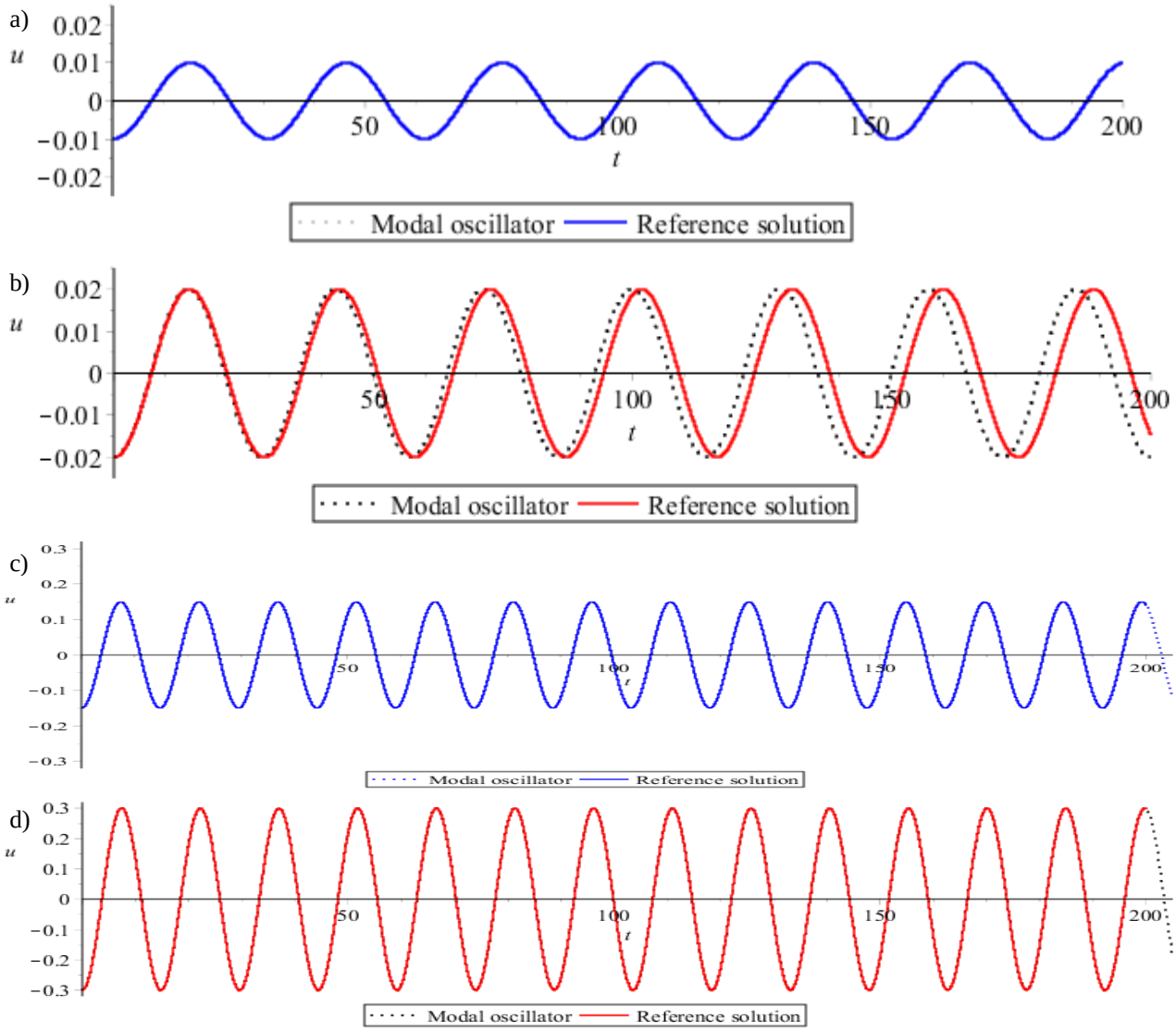

Figure 4:Comparative between modal oscillator and reference solution.
Modal oscillator defined in Eq. (25) with initial excitation conditions: a) u=-0,01 *e* v=0; b) u=-0,02 e v=0;
Modal oscillator defined in Eq. (26) with initial excitation conditions: c) u=-0,15 *e* v=0; d) u=-0,3 e v=0

It was found that as the initial amplitude of excitation of the system in each NNM increased, the discrepancy between the two solutions increased, i.e. for smaller excitations in each mode, the oscillators would better represent the behavior of the structure. This result was already expected because the surface of invariant manifold is tangent to the reference solution in the equilibrium position, and is closer for smaller amplitudes.

It is also noted that with the increase of the initial excitation of the first NNM, the frequency of the system increases indicating hardening of the system. For the second NNM, although the difference is not so noticeable the opposite occurs, the frequency of the system decreased with increasing excitation, indicating the phenomenon of softening.

The phase space of LNMs is closed, indicating the oscillation is cyclic, and the curves are ellipses, signaling that there are no changes between the modes in the vibration. The NNMs, as previously defined, are also periodic oscillations, so its curve should be closed. However, its shape may not be more elliptical, a fact that indicates its non-linearity.

In order to analyze the validity of the reduced order model in response to the numerical integration of the problem, phase spaces were elaborated for the two NNMs. Each orbit shown in Fig. 5 is generated from a given initial condition for the structure, showing the relation between modal displacement, u, and velocity, v, predicted for the free vibration behavior

of the structure. It can be seen from Figure 4 that by increasing the initial excitation of free vibration, the discrepancy between the curves increases.

The numerical integration curves that previously were practically coincident with the one of the modal oscillator begin to move away, showing that the use of the constraint equations to determine the NNMs lost their agreement with the real system. The validity of the reduced order model is not known a priori, it is necessary to compare the modal oscillators with the respective responses of the numerical solutions of the system of differential equations

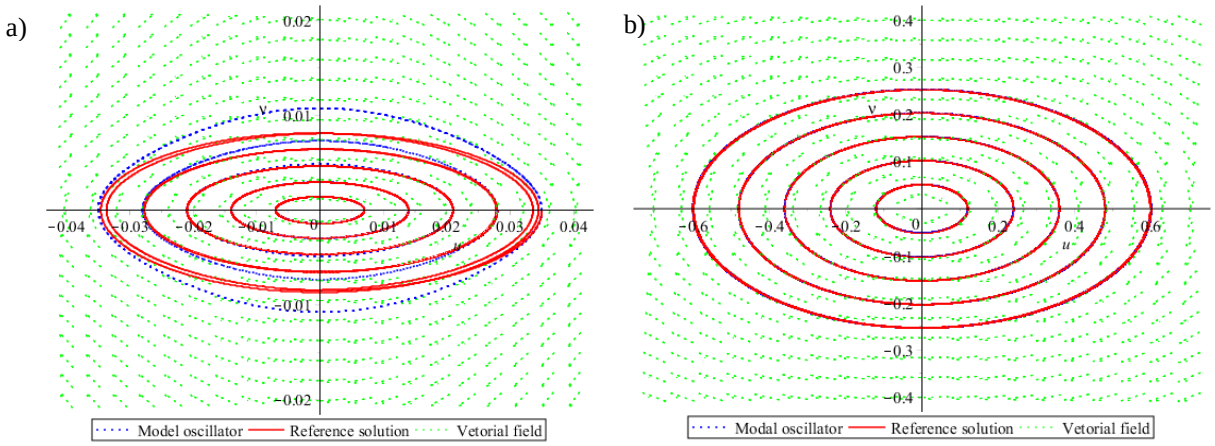

Figure 5: Phase space: a) first NNM; b) second NNM

For the reduced-order model of the first NNM, good agreement was obtained until rotations of the master degree of freedom close to 0.03 rad, as shown in Fig. 5 (a). Meaning that the rotation of the tower degree of freedom would be around 0.942 rad. For the reduced-order model of the second NNM, the agreement went beyond the physical limit of the system, as shown in Fig. 5 (b). The blue lines, which represent the modal oscillator, are visually imperceptible, indicating agreement of the oscillator with the numerical solution.

In linear systems, the frequency of vibration remains the same when the amplitude of the motion is changed, but for non-linear systems this correspondence is no longer valid. In order to determine the frequency-amplitude curve for each mode of vibration, the harmonic balance method was used in the reduced-order model system. The main idea behind the method is to "balance" the different harmonic terms arising from the equations of motion due to nonlinearity. A common approach is to neglect high-order terms, thereby solving a fundamental problem (Siller, 2004).

This method can give indications of loss or gain of stiffness in the system. Stiffness gain occurs when the system response exhibits an increase in frequency with an increase in amplitude of vibration, and loss of stiffness when the frequency of the NNM decreases when increasing the amplitude of vibration.

In this work, the resonance curves are obtained using one harmonic solution for a first estimative, where the following substitution is adopted on the modal 1-degree of freedom oscillators shown in Eqs. (25) and (26):

$$u(t) = X_1 \cos(\omega t). \tag{27}$$

The dimensionless parameter Ω is also introduced, standing for the relation between the vibration frequency of the system and the natural vibration frequency of the system related to the analyzed NNM, that means, ω/ω_1. The resulting equations for the two 1-DOF oscillators, with such substitutions, are than written as:

$$X_1{}^2 = \frac{0{,}039478\Omega^2 - 0{,}039478}{11{,}0932774125 + 9{,}267174427\Omega^2}; \tag{28}$$

$$X_1{}^2 = \frac{0{,}181721\Omega^2 - 0{,}181721}{-0{,}0148231 + 0{,}000408\Omega^2}. \tag{29}$$

Equation (28) shows hardening behavior with increasing motion amplitudes, as shown in Fig. 6(a). Equation (29) shows softening behavior with increasingly motion amplitudes on the system, as can be seen in Fig. 6(b).

In order to improve agreement with the reference solution of the first modal oscillator, a trigonometric term was also considered in the harmonic balance, as described in Eq. (30). The resolution procedure is analogous to that described above, but with consideration of one more variable.

$$u(t) = X_1 \cos(\omega t) + X_2 \cos(3\omega t). \tag{30}$$

In Figure 6 the reference solutions are compared with the responses obtained from the modal oscillators. It is observed that for the first NNM, the rotations up to 0,02 rad of the master degree of freedom showed good compliance. The use of one more harmonic term in the harmonic balance method slightly improved the agreement. The consonance of the second NNM was adequate up to rotations greater than 0,3 rad of the master degree of freedom, being valid for the physical domain of the problem.

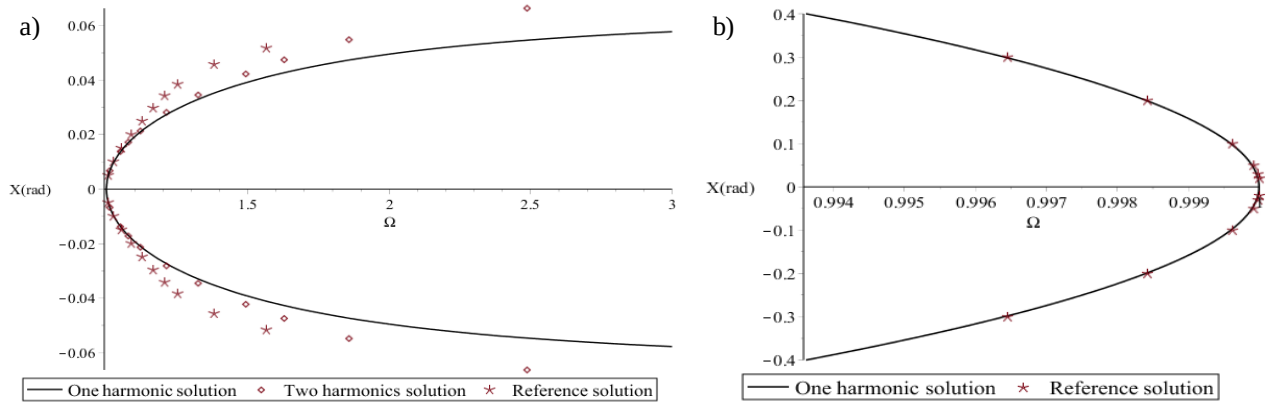

Figure 6: Ressonance curves: a) first NNM; b) second NNM

It can be noted that for the first NNM an increase in system stiffness occurs, i.e., the vibration frequency increases with increasing excitation amplitude. In the second NNM, the opposite occurs, the system loses stiffness, signaling that for greater excitations, the frequency decreases. Both curves are symmetric, since the nonlinearity is due only to cubic terms.

The energy of the system is calculated by replacing the solution allowed by the harmonic balance method, Eq. (27), in the equation of total potential energy, given in Eq (5). The energy variation of the system is shown with semi-logarithmic axes in Fig. 7, with energy increase for the first NNM and energy decrease for the second NNM. There are also represented the energy of the linearized system, where the horizontal line represents the independence of the system's natural frequency to the given energy amount dispose to the system vibration.

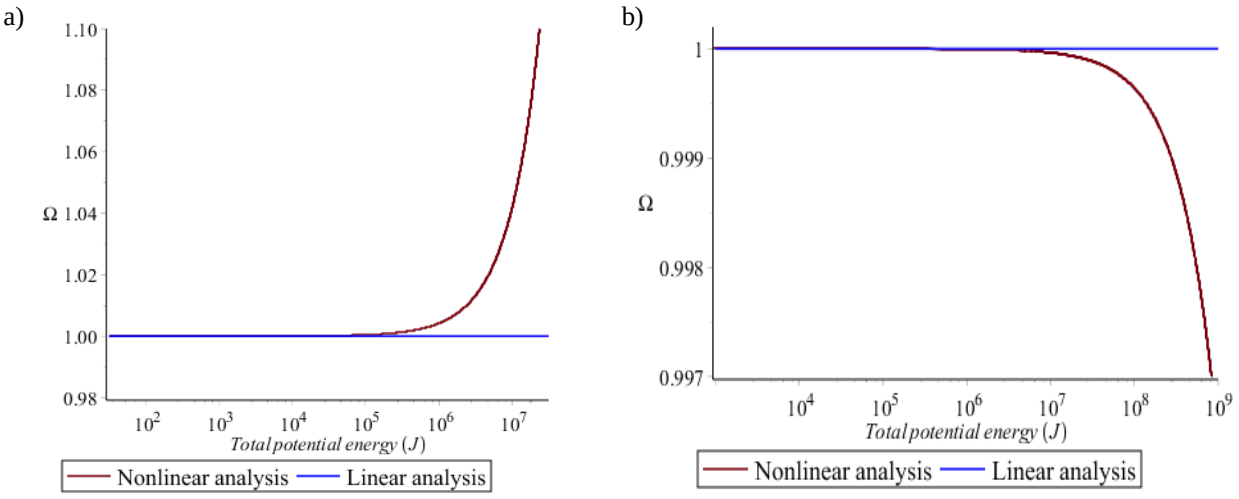

Figure 7: Frequency-energy curves: a) first NNM; b) second NNM

5. CONCLUSIONS

The nonlinear dynamic analysis of a spar type floating offshore wind turbine in free vibration was carried out in order to identify and analyze the nonlinear phenomena present in the system. For that, a discrete system with two degrees of freedom, the pitching rotation of the platform and of the tower was considered.

The invariant manifold approach was used in the expanded equation of the system in Taylor series up to the third term. It was verified that the identification of the NNMs constituted of a useful technique in the prediction of structures's behavior under determined conditions through the analysis of the response in time and phase space of the system.

The modal oscillators obtained were used to study the non-damped free vibration behavior of the system. It was analyzed phase spaces of the master degree (degree relative to platform pitching rotation) and the frequency-amplitude curves achieved through the harmonic balance method . The responses were compared with the reference solution to verify the representativeness of the reduced order model oscillator. The response of the first NNM was compatible to the reference solution until amplitude values of the master degree of freedom near of 0,025 rad, indicating hardening and increase of the total potential energy of the system. However, the modal oscillators of the second NNM obtained a good precision until master degree rotations above 0,3 rad, sufficient value to guarantee the use in all the domain of physical analysis of the system. And, unlike the previous case, the second NNM showed a decrease in the vibration frequency for excitation with higher amplitudes, and decrease of the potential energy with increasing frequency.

6. REFERENCES

Apiwattanalunggarn, P. *et al.*, 2003, "Finite-element-based nonlinear modal reduction of a rotating beam with large-amplitude motion". Journal of Vibration and Control, v. 9, p. 235–263.

Gavassoni, E., 2007."Modelos Discretizados de Dimensão Reduzida para Análise Dinâmica Não linear de Vigas e Pórticos Planos", 136 f. Master dissertation – PUC-RIO, Rio de Janeiro.

GWEC., 2018. "A Snapshot of Top Wind Markets in 2017: Offshore Wind". pp. 54-63.

Harriger, E., 2011," Dynamis analysis of a 5 megawatt offshore floating wind turbine". Master dissertation, University of California.

Jonkman, J. M., 2007. "Dynamics modeling and loads analysis of an offshore floating wind turbine". National Renewable Energy Laboratory – Technical report.

Jonkman, J., 2010 "Definition of the Floating System for Phase IV of OC3 Definition of the Floating System for Phase IV of OC3". National Renewable Energy Laboratory – Technical report.

Jonkman, J; Musial, W., 2010. "Offshore code comparison collaboration (OC3) for IEA wind task 23 offshore wind technology and deployment". National Renewable Energy Laboratory – Technical report.

Kerschen, G. et al., 2006. "Past, present and future of nonlinear system identification in structural dynamics". Mechanical Systems and Signal Processing, v. 20, n. 3, p. 505–592.

Musial, W; Butterfield, N., 2006. "Energy From Offshore Wind". Offshore Technology Conference, pp.11.

Pesheck, E. et al., 2001. " Nonlinear Modal Analysis of Structural Systems Using Multi-Mode Invariant Manifolds". Springer Verlag, n. Nonlinear Dynamics, p. 188–203.

Shaw, S. W.; Pierre, C. 1993. " Normal modes for nonlinear vibratory systems". Journal of Sound and Vibration, v.164, n. 1, pp. 85-124.

Siller, H. R. E., 2004. "Non-linear modal analyis methods for engineering structures". 242 f. Doctor thesis– Imperial College London, University of London, London.

Vakakis, A., 1997. "Non-linear normal modes (NNMs) and their applications in vibration theory: An overview". Mechanical Systems and Signal Processing, v. 11, n. 1, p. 3–22, 1997.

Wang, X. et al., 2018. "A review on recent advancements of substructures for offshore wind turbines". Energy Conversion and Management, v. 158, n. September 2017, pp. 103–119.

7. RESPONSIBILITY NOTICE

The authors are the only responsible for the printed material included in this paper.